Electronic Supplementary Material (ESI) for Physical Chemistry Chemical Physics.

Supporting Information for

Study of pnictides for photovoltaic applications

Jayant Kumar, and Gopalakrishnan Sai Gautam*

Department of Materials Engineering, Indian Institute of Science, Bengaluru 560012, India

*E-mail: saigautamg@iisc.ac.in

Potentials used

To describe the core electrons of each atomic species, the following projector augmented wave potentials were used: Ca_sv 06Sep2000, Sr_sv 07Sep2000, Zn 06Sep2000, N 08Apr2002, and P 06Sep2000.

Crystal structure and electronic structure of pnictides

Table S1: Lattice parameters and lattice angles, as calculated by the strongly constrained and appropriately normed (SCAN) functional are listed for all structures considered in this work. Structural origin column indicates whether the structure was obtained from the inorganic crystal structure database (ICSD) or via theoretical substitution. Space group column indicates the space group as obtained from ICSD or corresponding to the template structure for theoretical configurations. Heyd-Scuseria-Ernzerhof (HSE06) hybrid functional calculated band gaps are listed alongside experimental (Expt.) values for each structure. The references corresponding to experimental band gaps are included in **Table 2** of the main text.

Compounds	**Structural origin**	**Space group**	**Lattice parameters**						**E_g (eV)**	
			Edge lengths (Å)			**Lattice angles (°)**			**Calculated**	**Expt.**
			a	***b***	***c***	***α***	***β***	***γ***		
Binaries										
Ca_3N_2	ICSD	$Ia\bar{3}$	11.41	11.41	11.41	90.00	90.00	90.00	1.75	1.90
Ca_3P_2		$P6_3/mcm$	8.44	8.44	6.28	89.99	90.00	120.00	0.59	-
Sr_3N_2	Theoretical	$Ia\bar{3}$	12.26	12.26	12.26	90.00	90.00	90.00	0.93	-
Sr_3P_2	ICSD	$I\bar{4}3d$	24.11	8.11	8.11	110.52	109.14	109.14	0.38	-
Zn_3N_2		$Ia\bar{3}$	9.71	9.71	9.71	90.00	90.00	90.00	0.64	1.23
Zn_3P_2		$P4_2/nmc$	8.02	8.02	11.26	90.00	90.00	90.00	0.90	1.46
Ternaries										
$CaSr_2N_2$	Theoretical	$P4_2/nmc$	8.46	8.46	12.06	90.00	90.00	90.00	1.22	-
$CaSr_2P_2$			10.48	10.48	11.39	89.99	89.99	90.00	1.75	-
$SrZn_2N_2$		$P\bar{3}m1$	3.53	3.53	6.22	89.99	89.99	120.00	1.39	1.60
$SrZn_2P_2$	ICSD		4.07	4.07	7.10	89.99	89.99	119.99	1.18	-
$CaZn_2N_2$	Theoretical		3.44	3.44	5.96	90.00	89.99	120.00	1.65	1.90
$CaZn_2P_2$	ICSD		4.00	4.00	6.80	90.00	90.00	120.00	1.23	-
$SrCa_2N_2$	Theoretical		3.98	3.98	6.73	90.00	89.99	119.99	2.36	-
$SrCa_2P_2$			4.70	4.70	7.47	89.99	90.00	120.00	2.12	-
$ZnCa_2N_2$	ICSD	$I4/mmm$	3.57	3.57	12.49	90.00	90.00	90.00	1.40	1.60
$ZnCa_2P_2$	Theoretical		4.16	4.16	14.97	90.00	90.00	90.00	0.80	-
$ZnSr_2N_2$	ICSD		3.85	3.85	12.77	90.00	90.00	90.00	1.38	-
$ZnSr_2P_2$		$P6_3/mmc$	4.20	4.20	8.38	90.00	90.00	120.08	0.12	-
Quaternaries										
$CaSrZnN_2$	Theoretical	$I4/mmm$	3.73	3.73	12.62	90.00	90.00	90.00	1.33	-
$CaSrZnP_2$		$P\bar{3}m1$	4.39	4.39	7.32	89.99	90.00	119.99	1.41	-

Chemical potential ranges for defect calculations

Table S2: Range of chemical potentials (μ) of different elements (in units of eV) in candidate nitrides and phosphides, as obtained from respective 0 K phase diagrams. Note that each compound considered is thermodynamically stable over the specified range of chemical potentials for each element. The zero of the chemical potentials of all species are referenced to the corresponding pure elements in their bulk ground state forms.

Compounds	Elements	Chemical potentials (eV)	
		Maximum (μ_{max})	Minimum (μ_{min})
$SrZn_2N_2$	Sr	-1.52	-2.14
	Zn	0	-0.12
	N	0	-0.34
$SrZn_2P_2$	Sr	-1.10	-2.95
	Zn	0	-0.59
	P	-9.56	-10.80
$CaZn_2P_2$	Ca	-1.10	-2.99
	Zn	0	-0.60
	P	-9.53	-10.82
$ZnCa_2N_2$	Zn	0	-0.99
	Ca	-0.49	-2.19
	N	0	-1.72
$ZnSr_2N_2$	Zn	0	-0.93
	Sr	-0.24	-1.76
	N	-0.09	-1.62

Our choice of chemical potentials is based on the 0 K phase diagram (**Figure 2** of the main text). Consider a candidate material, say $CaZn_2P_2$, whose relevant convex hull is Ca-Zn-P (**Figure 2e**). Being a stable phase at 0 K, $CaZn_2P_2$ is part of several Gibbs triangles (analogous to tie-lines in binary phase diagrams) of the Ca-Zn-P system, namely $CaZn_2P_2$-Zn-Zn_3P_2, $CaZn_2P_2$-Zn_3P_2-ZnP_2, $CaZn_2P_2$-ZnP_2-Ca_5P_8, $CaZn_2P_2$-Ca_5P_8-CaP, $CaZn_2P_2$-CaP-Ca_3P_2, and $CaZn_2P_2$-Ca_3P_2-Zn. Each of these Gibbs triangles exhibit a unique P, Zn (and hence Ca) chemical potential (μ) since we have three phases that are in equilibrium in a ternary system at constant temperature and pressure. Upon evaluating the μ for each Gibbs triangle containing $CaZn_2P_2$, based on SCAN-calculated total energies, we get a range of μ_P, μ_{Zn}, and μ_{Ca} over which $CaZn_2P_2$ is stable. Subsequently, we identify the maximum and minimum μ for a given element and use these values to determine the range of defect formation energies for a defect involving the element. For example, the relevant range of μ_{Zn} for the formation of a Zn vacancy within $CaZn_2P_2$ is 0 eV (maximum) and -0.59 eV (minimum), where the zero of μ_{Zn} is referenced to the SCAN-calculated total energy of pure Zn in its bulk hexagonal-close-packed ground state structure. Similar evaluation of μ ranges relevant for point defect formation have been done before for compound semiconductors, such as Cu_2ZnSnS_4.[1]

Convergence of total energies

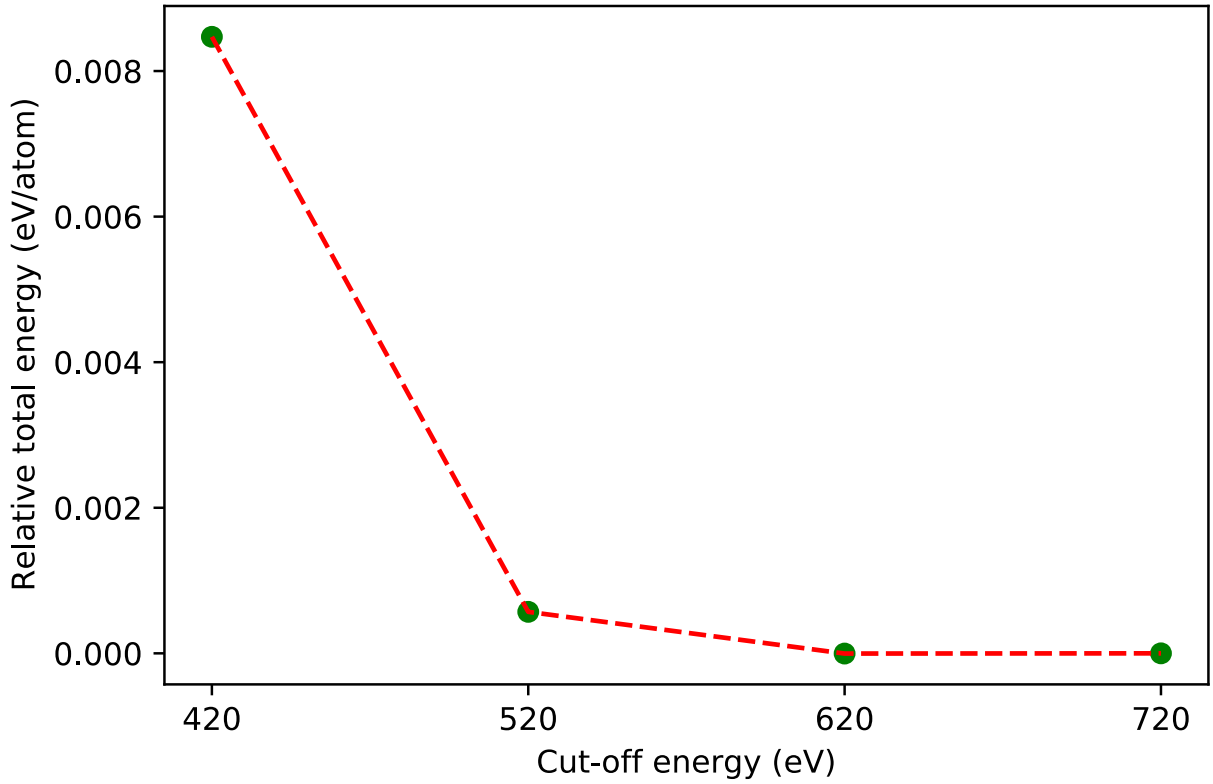

Figure S1: Plot showing the variation of density functional theory (DFT)-calculated total energy of $ZnCa_2N_2$ with respect to the kinetic energy cut-off used for the plane-wave basis. The total energies are references relative to the total energy at the 720 eV cut-off. We used the SCAN functional for calculating the total energies at various cut-off values. We find that the total energy at a 520 eV cut-off converges to within 1 meV/atom compared to the total energy at a 720 eV cut-off.

Theoretical structures of pnictides

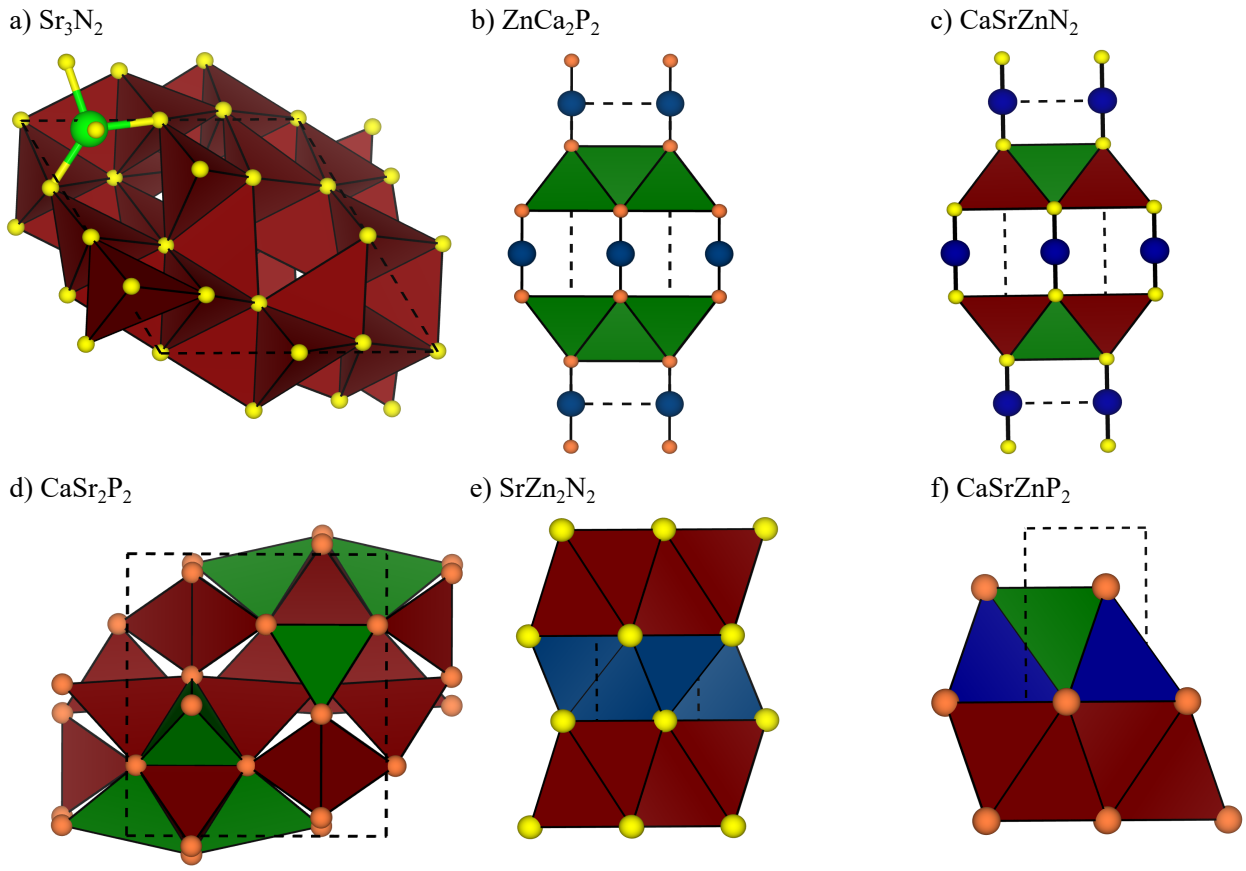

Figure S2: Initial theoretical structures of pnictides, including a) $Ia\bar{3}$-Sr_3N_2, b) $I4/mmm$-$ZnCa_2P_2$, c) $I4/mmm$-$CaSrZnN_2$, d) $P4_2/nmc$-$CaSr_2P_2$ (and $CaSr_2N_2$), e) $P\bar{3}m1$-$SrZn_2N_2$ ($CaZn_2N_2$, $SrCa_2N_2$, and $SrCa_2P_2$), and f) $P\bar{3}m1$-$CaSrZnP_2$. All space groups indicated are for the corresponding template structures. The open polyhedron in panel a shows the tetrahedral coordination of the Sr atom in Sr_3N_2. Color codes: Ca – green, Sr – brown, Zn – blue, N – yellow, and P – orange.

For compounds whose structures are not available in the inorganic crystal structure database (ICSD[2]), we used the ordered structures with unique space groups in **Table 1** of the main text (marked with "*" in the "Space group" column) as templates to derive the new initial structures. Specifically, we used the unit cells of Zn_3P_2 ($P4_2/nmc$), $ZnCa_2N_2$/$ZnSr_2N_2$ ($I4/mmm$), and $CaZn_2P_2$/$SrZn_2P_2$ ($P\bar{3}m1$) as the templates, all of which exhibit 3 distinct cation sites that can be interchanged. For example, substituting all Ca with Sr in $CaZn_2P_2$ (1a site) and $ZnCa_2N_2$ (4e sites) lead to identical Sr-containing structures, namely, $SrZn_2P_2$ and $ZnSr_2N_2$, respectively. Thus, Ca and Sr sites can be used for the occupation of either cation. Römer et. al. studied different theoretical structures for Sr_3N_2, such as anti-B-sesquioxide, anti-Rh_2O_3-II, hexagonal $P6_3/mmc$, and anti-bixbyite $Ia\bar{3}$.[3] Among these structures, the anti-bixbyite was found

to have the lowest energy, similar to the binary Ca and Zn nitrides. Hence, we used the Ca_3N_2 structure as a template to initialize the anti-bixbyite Sr_3N_2 structure by substituting Ca with Sr.

For generating the ternary nitride structures, we did not use the $Ia\bar{3}$-Ca_3N_2 or Zn_3N_2 structures as templates since the framework contains 24 distinct cation sites, which presents a combinatorial limitation (i.e., large number of unique configurations to consider) to computational substitution. Similarly, we did not consider the Sr_3P_2, Ca_3P_2, and $ZnSr_2P_2$ disordered structures as templates due to the combinatorial limitation. The DFT-calculated energies for the different initial configurations considered and the initial configurations of the ground states for all theory-derived structures are compiled in **Table S3, S4** and **Figure S2**.

As an example of our procedure for theoretically deriving structures, consider the case of $CaSr_2P_2$. Here, we generated three sets of structures, by substituting Zn and N with Ca and P in $ZnSr_2N_2$ (i.e., the Sr sites left as-is), replacing Sr and Zn with Ca and Sr in $SrZn_2P_2$ (i.e., 1a sites are occupied by Ca and 2d sites are occupied by Sr after replacement, which ensures correct stoichiometry of Ca and Sr in $CaSr_2P_2$), and exchange two 8g sites of Zn with Sr and one 8g site with Ca in Zn_3P_2. The aforementioned substitutions gave rise to 1, 1, and 3 symmetrically distinct configurations of $CaSr_2P_2$ as derived from $ZnSr_2N_2$, $SrZn_2P_2$, and Zn_3P_2, respectively, out of which the DFT-calculated ground state was one of the configurations derived from Zn_3P_2 (**Figure S2d**). Among the theoretical ternaries (see **Table S3** and **Figure S2**), the DFT-calculated ground state configurations of $ZnCa_2P_2$ (**Figure S2b**) and $CaSr_2N_2$ (**Figure S2d**) were derived from $ZnCa_2N_2$ ($I4/mmm$), and Zn_3P_2 ($P4_2/nmc$), respectively, while the ground states of the other ternaries ($CaZn_2N_2$, $SrZn_2N_2$, $SrCa_2N_2$, and $SrCa_2P_2$, **Figure S2e**) were based on $CaZn_2P_2$/$SrZn_2P_2$ ($P\bar{3}m1$). Notably, our ground state configuration of $SrZn_2N_2$ and $CaZn_2N_2$ (derived from a $P\bar{3}m1$ space group) are consistent with previous theoretical studies as well,[4] highlighting the robustness of our substitution strategy.

For the quaternaries $CaSrZnN_2$ and $CaSrZnP_2$ (see **Table S4** and **Figure S2**), we derived the theoretical structures by substitution that was done analogously to the ternary compounds. For example, to obtain $CaSrZnP_2$ configurations, we substituted 1 8g site each with Sr and Ca in Zn_3P_2, considered Ca, Sr, and Zn occupying the 1a and 2d sites in $CaZn_2P_2$ (i.e., each cation is allowed to occupy one of the distinct Wyckoff sites), and the three cations residing in the 2a and 4e sites and all N replaced with P in $ZnSr_2N_2$. Such substitution resulted in 6, 3, and 3 unique configurations of $CaSrZnP_2$ derived from Zn_3P_2, $CaZn_2P_2$, and $ZnSr_2N_2$, respectively, out of which the DFT-

calculated ground state was based on the ternary-$CaZn_2P_2$ (**Figure S2f**). The $ZnSr_2N_2$ ternary formed the ground state template for $CaSrZnN_2$ quaternary (**Figure S2c**).

Table S3: Initial structures of ternary pnictides derived from structural templates. Each Sr. No. within a space group indicates different possible, symmetrically-distinct cation-vacancy arrangements. The relative energy (in eV/f.u.) column indicates the calculated total energy (using density functional theory) of template structures relative to the ground state configuration (in bold font).

Compounds	Template structure	Space group	Sr. No.	Relative energy (eV/f.u.)
$ZnCa_2P_2$	Zn_3P_2	$P4_2/nmc$	1	0.21
			2	1.20
			3	0.24
	$ZnCa_2N_2$	$\boldsymbol{I4/mmm}$	**4**	**0**
	$CaZn_2P_2$	$P\bar{3}m1$	5	0.08
$CaZn_2N_2$	Zn_3P_2	$P4_2/nmc$	1	1.34
			2	0.97
			3	1.34
	$ZnCa_2N_2$	$I4/mmm$	4	3.49
	$CaZn_2P_2$	$\boldsymbol{P\bar{3}m1}$	**5**	**0**
$SrZn_2N_2$	Zn_3P_2	$P4_2/nmc$	1	1.32
			2	1.01
			3	1.44
	$ZnSr_2N_2$	$I4/mmm$	4	3.54
	$CaZn_2P_2$	$\boldsymbol{P\bar{3}m1}$	**5**	**0**
$SrCa_2N_2$	Zn_3P_2	$P4_2/nmc$	1	0.38
			2	0.16
			3	0.32
	$ZnCa_2N_2$	$I4/mmm$	4	1.39
	$SrZn_2P_2$	$\boldsymbol{P\bar{3}m1}$	**5**	**0**
$SrCa_2P_2$	Zn_3P_2	$P4_2/nmc$	1	0.62
			2	0.59
			3	0.62
	$ZnCa_2N_2$	$I4/mmm$	4	1.81
	$SrZn_2P_2$	$\boldsymbol{P\bar{3}m1}$	**5**	**0**
$CaSr_2N_2$	Zn_3P_2	$\boldsymbol{P4_2/nmc}$	**1**	**0**
			2	0.28
			3	0.02
	$ZnSr_2N_2$	$I4/mmm$	4	0.92
	$SrZn_2P_2$	$P\bar{3}m1$	5	1.05
$CaSr_2P_2$	Zn_3P_2	$\boldsymbol{P4_2/nmc}$	1	0.08
			2	0.40
			3	**0**
	$ZnSr_2N_2$	$I4/mmm$	4	1.04
	$SrZn_2P_2$	$P\bar{3}m1$	5	0.08

Table S4: Initial structures of quaternary pnictides derived from available structural templates. Columns displayed are similar to those used in **Table S3**.

Compounds	Template structure	Space group	Sr. No.	Relative energy (eV/f.u.)
$CaSrZnN_2$	Zn_3P_2	$P4_2/nmc$	1	1.01
			2	2.18
			3	1.14
			4	2.01
			5	0.95
			6	0.90
	$ZnSr_2N_2$	$\boldsymbol{I4/mmm}$	**7**	**0**
			8	3.89
			9	3.46
	$CaZn_2P_2$	$P\bar{3}m1$	10	0.88
			11	0.90
			12	0.01
$CaSrZnP_2$	Zn_3P_2	$P4_2/nmc$	1	0.45
			2	1.71
			3	0.58
			4	1.43
			5	0.45
			6	0.33
	$ZnSr_2N_2$	$I4/mmm$	7	3.25
			8	3.28
			9	2.95
	$CaZn_2P_2$	$\boldsymbol{P\bar{3}m1}$	10	0.15
			11	**0**
			12	0.25

Density of states of nitrides and phosphides

We present the plots showing density of states (DOS) of all the compounds obtained using the SCAN and hybrid (HSE06) functionals.

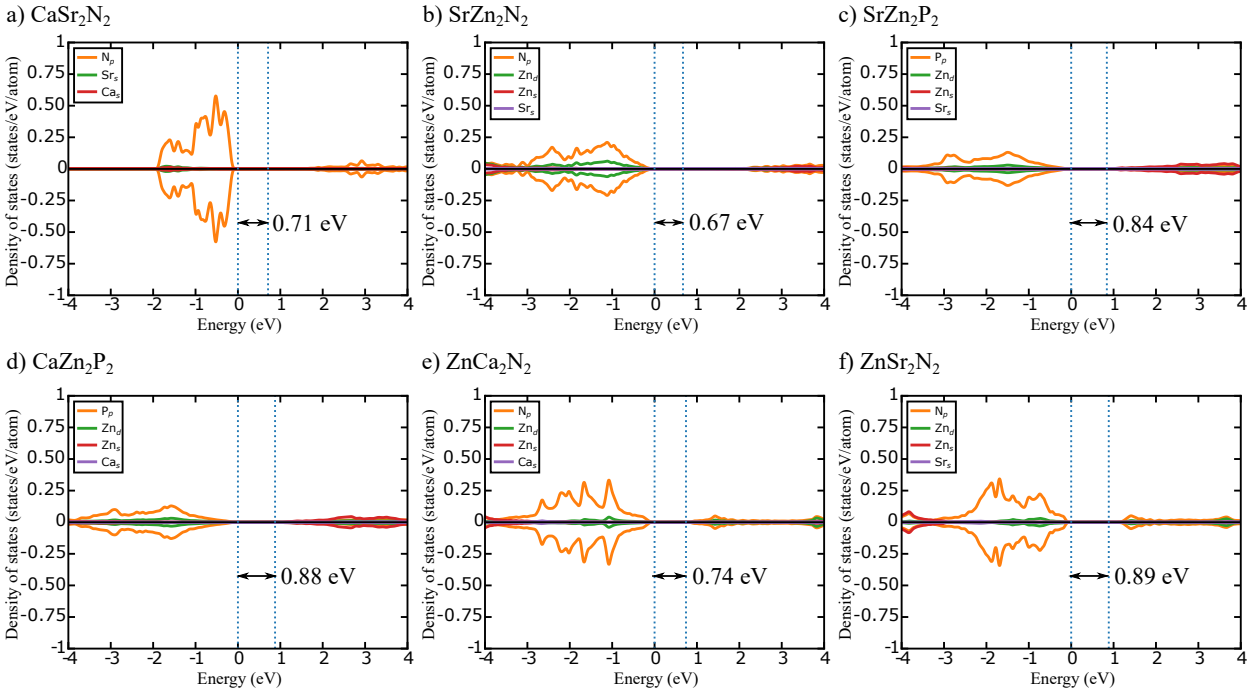

Figure S3: SCAN-calculated DOS for ternary candidate pnictides (i.e., same compounds as in **Figure 2** of the manuscript). Text annotation in each panel indicates the calculated band gap with the dotted blue lines highlighting the band edges.

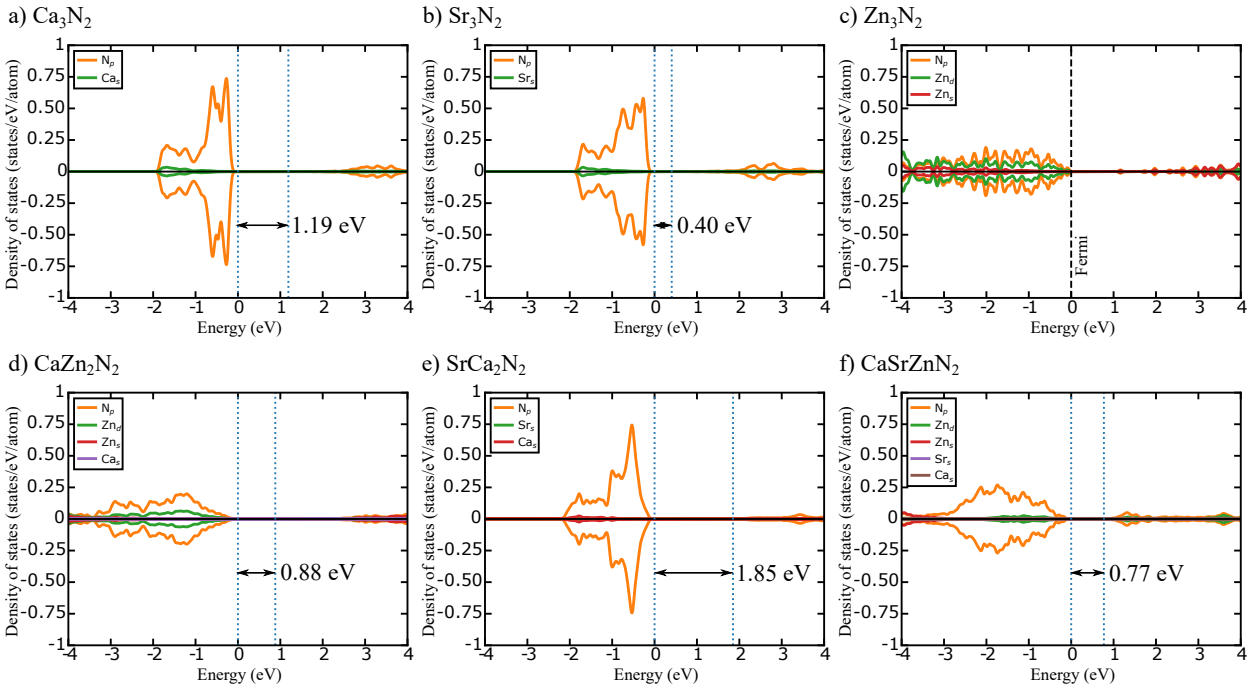

Figure S4: SCAN-calculated DOS for non-candidate nitrides. Annotations in each panel are similar to **Figure S3**. Zn_3N_2 is metallic, so the dashed black line indicates the Fermi level.

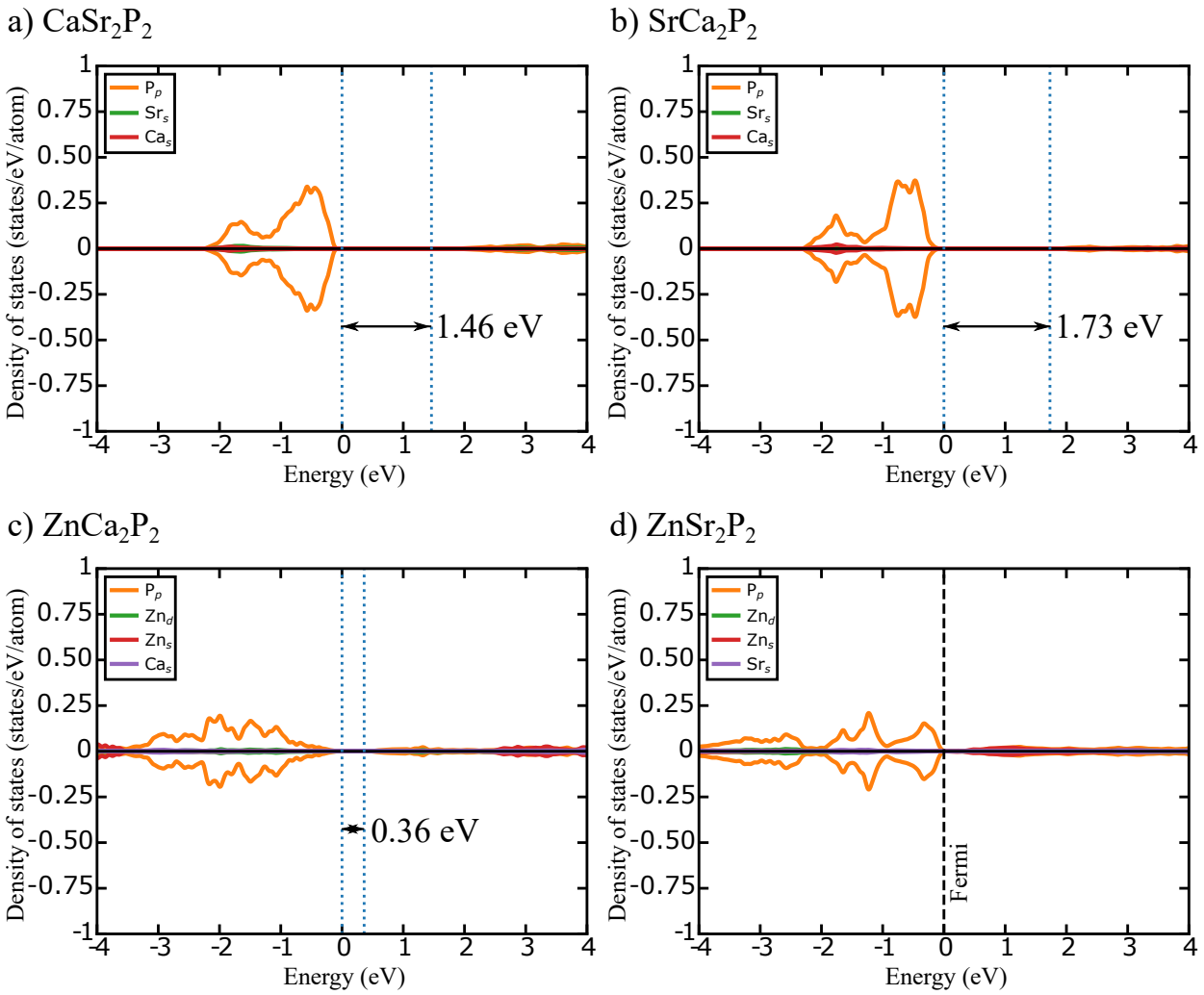

Figure S5: SCAN-calculated DOS for non-candidate ternary phosphides. Annotations in each panel are similar to **Figure S3**. $ZnSr_2P_2$ is metallic.

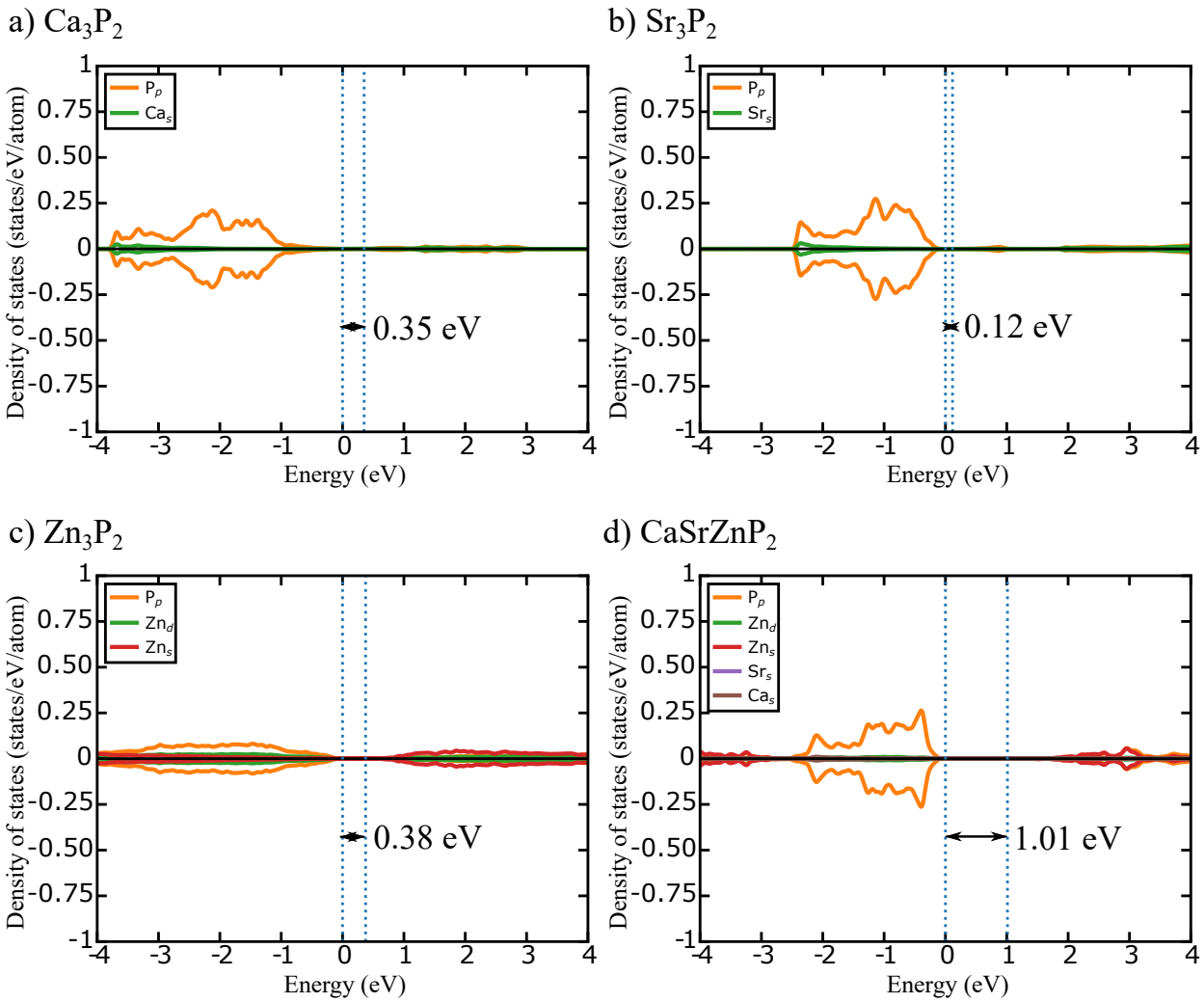

Figure S6: SCAN-calculated DOS for non-candidate binary and quaternary phosphides. Annotations in each panel are similar to **Figure S3**.

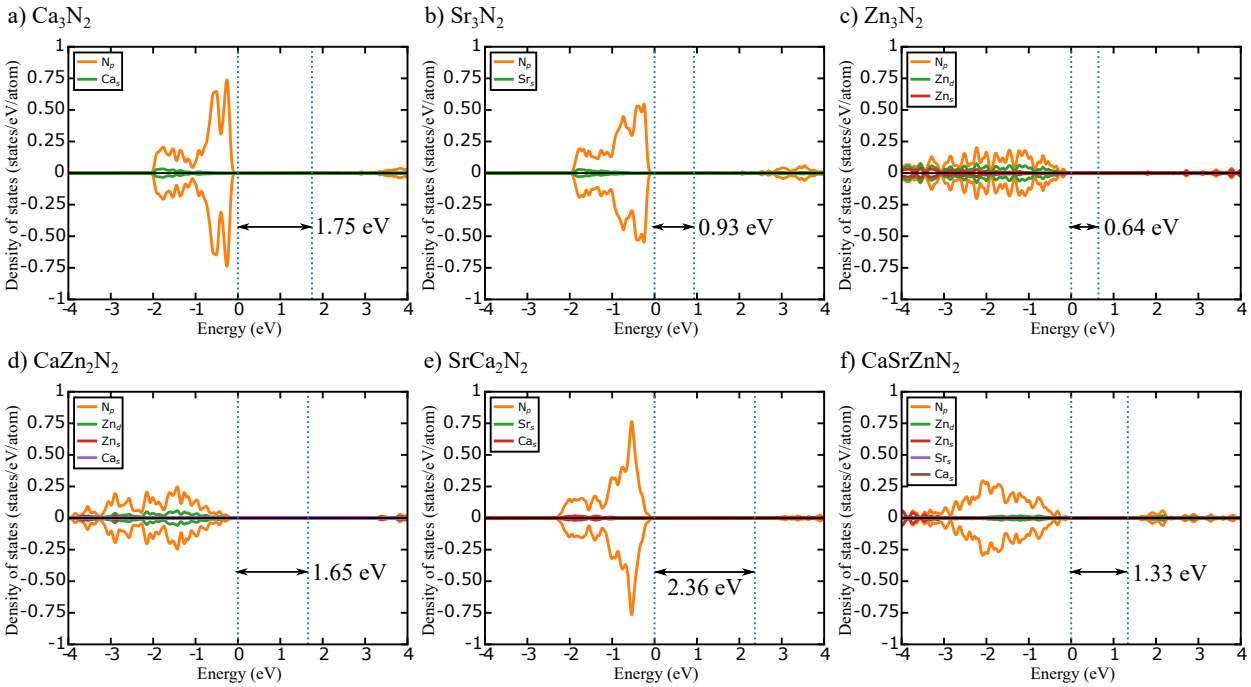

Figure S7: HSE06-calculated DOS for non-candidate nitrides. Annotations in each panel are similar to **Figure S3**.

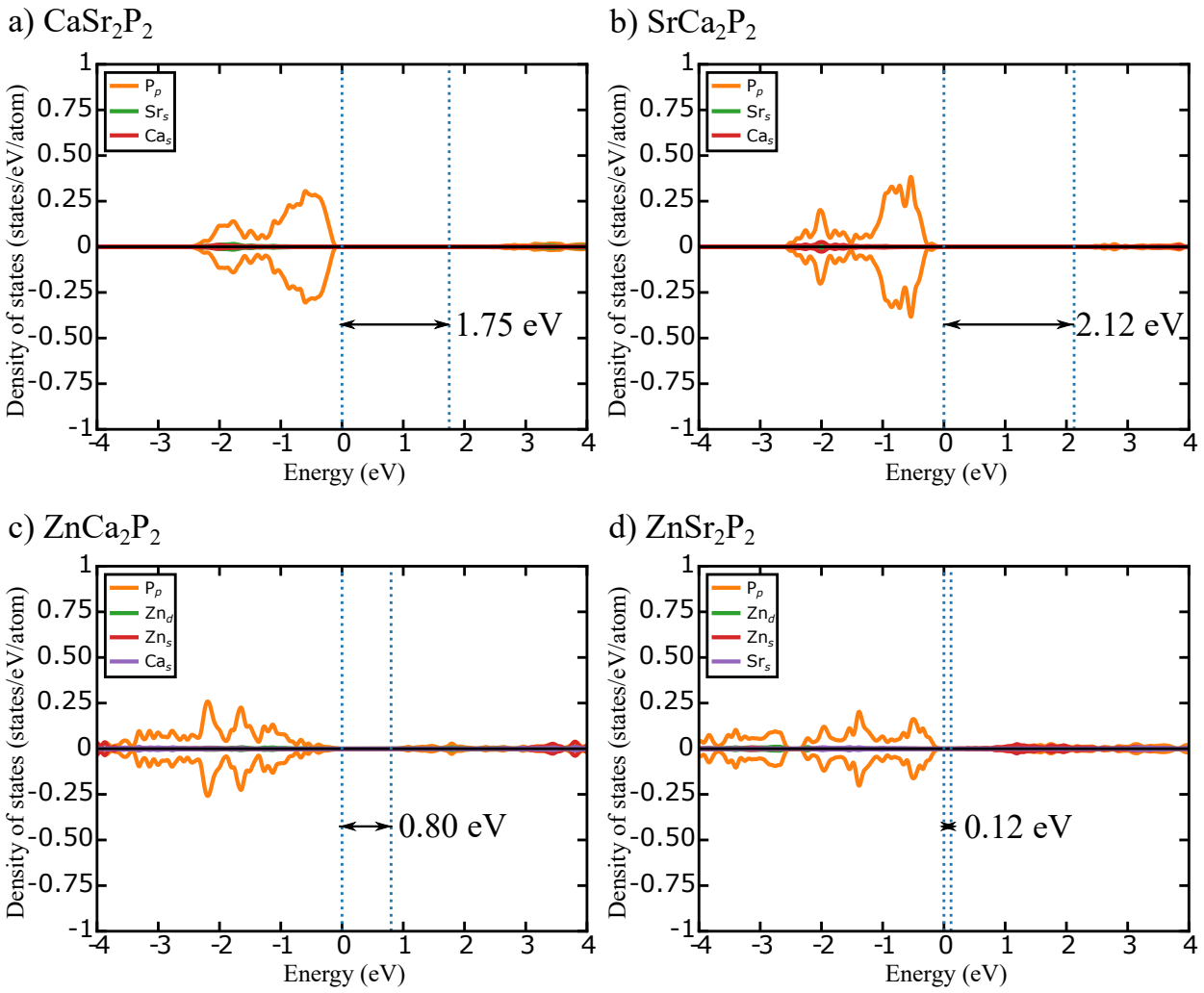

Figure S8: HSE06-calculated DOS for non-candidate ternary phosphides. Annotations in each panel are similar to **Figure S3**.

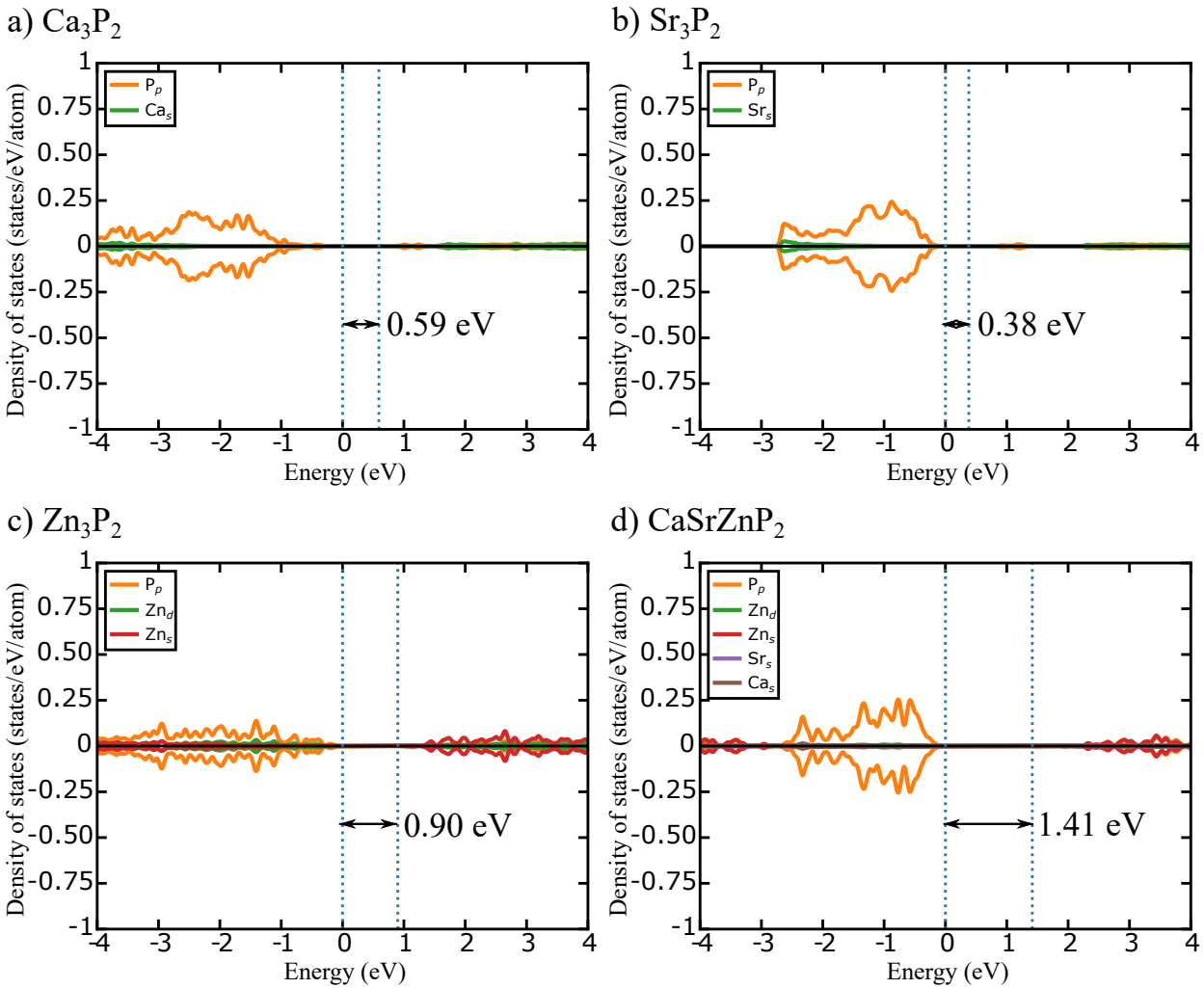

Figure S9: **HSE06**-calculated DOS for non-candidate binary and quaternary phosphides. Annotations in each panel are similar to **Figure S3**.

Band structures of candidate pnictides

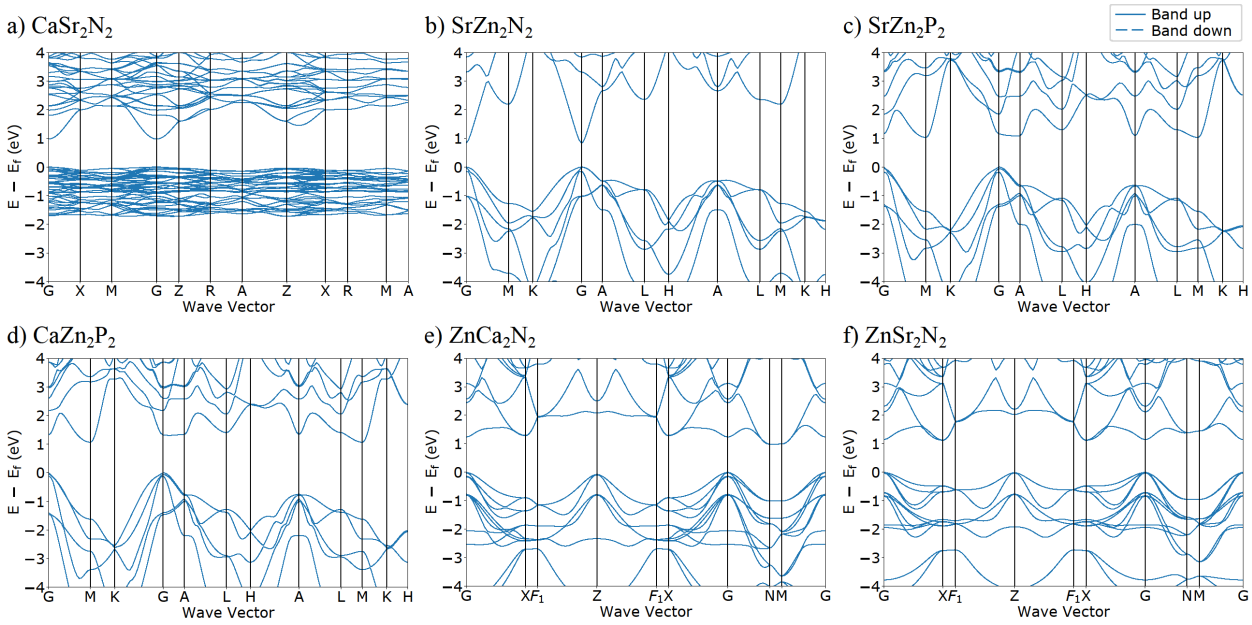

Figure S10: SCAN-calculated band structures for the six candidate pnictides identified in this work.

Correlation between calculated formation energies and band gaps

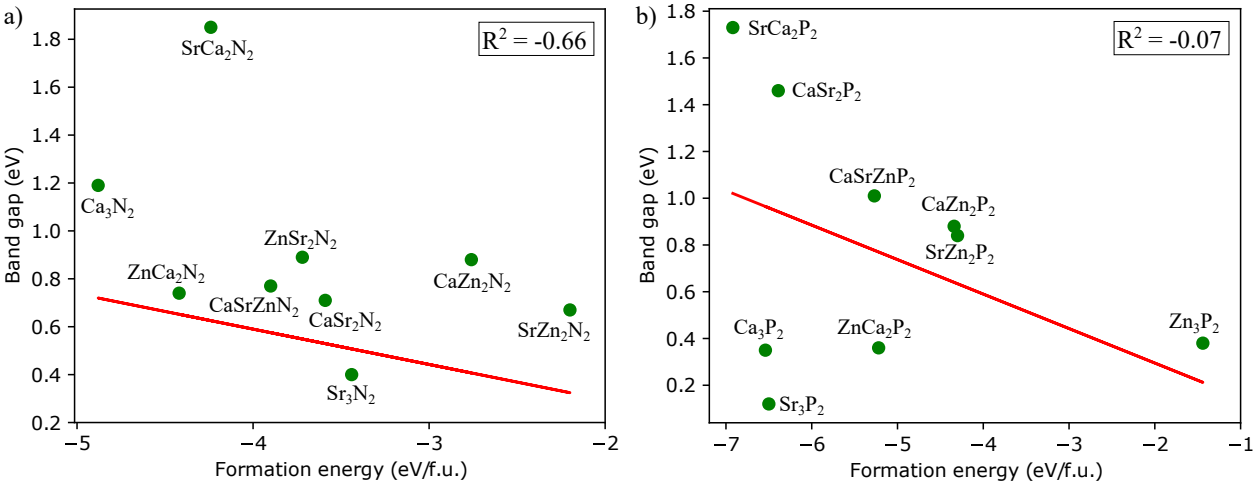

Figure S11: SCAN-calculated band gaps are plotted with respect to the SCAN-calculated formation energies of the (a) nitrides and (b) phosphides considered in this work. Formation energies for each compound are calculated with respect to their elements. We did not include the two pnictides which SCAN predicts to be metallic in the above plot. Importantly, we find marginal correlation between calculated formation energies and band gaps in case of nitrides, while any correlation between the two quantities is negligible in phosphides.

Phonon calculations and thermal properties

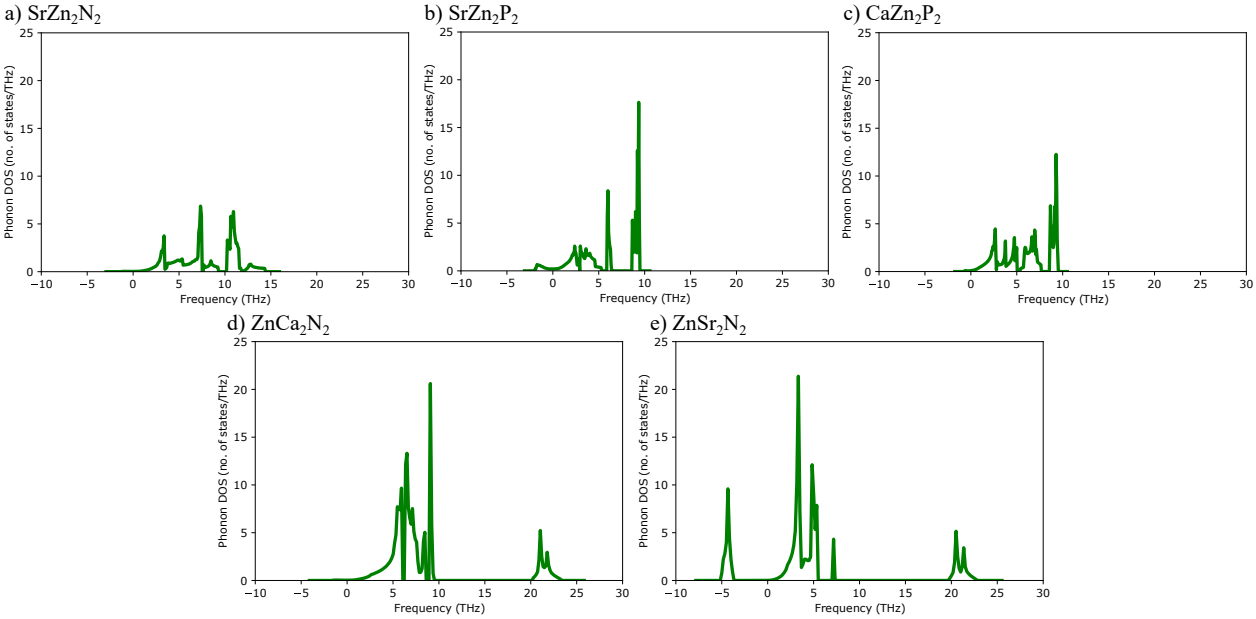

Figure S12: Phonon density of states calculated for the five candidate pnictides considered in this work, using SCAN. Negative frequencies correspond to imaginary phonon modes.

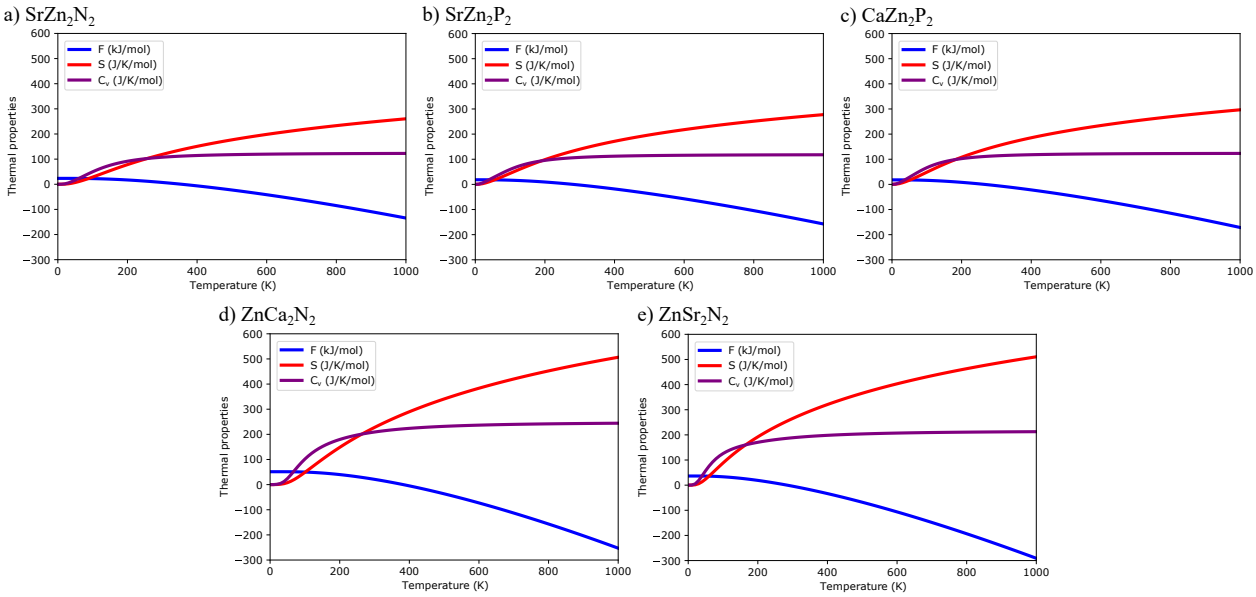

Figure S13: Thermal properties, including the Helmholtz energy (F, blue lines), entropy (S, red lines), and specific heat at constant volume (C_v, purple lines) are plotted as a function of temperature for the five candidate pnictides. Thermal properties were calculated based on SCAN-phonon calculations, where the imaginary phonon modes were ignored.

References

1. Gautam, G. S., Senftle, T. P. & Carter, E. A. Understanding the Effects of Cd and Ag Doping in Cu_2ZnSnS_4 Solar Cells. *Chem. Mater.*, **30**, 4543-4555 (2018).

2. Hellenbrandt, M. The inorganic crystal structure database (ICSD) - Present and future. *Crystallogr. Rev.* **10**, 17–22 (2004).

3. Rebecca Römer, S., *et al.*,. Group II element nitrides M_3N_2 under pressure: A comparative density functional study. *Phys. Status Solidi Basic Res.* **246**, 1604–1613 (2009).

4. Kikuchi, R. *et al.* $SrZn_2N_2$ as a Solar Absorber: Theoretical Defect Chemistry and Synthesis by Metal Alloy Nitridation. *Chem. Mater.* **33**, 2864–2870 (2021).